Ultra-precision Machining of Surfaces of Elements of Devices from Optical Materials

S. V. Grubiy, M. A. Shavva and V. V. Lapshin

Abstract Optical materials are widely used in the composition of modern engineering products and aerospace and electronics industries. At the same time, optical surface processing quality is ensured only with the use of diamond cutting tools and ultra-precision ultra-rigid equipment. In addition, it is necessary to provide cutting conditions in the nanoscale thickness range of the cut layer. The results of theoretical and experimental studies aimed at improving the performance, accuracy, and quality of machining surfaces of elements of devices from optical materials (reducing the roughness and depth of fractured layer), potassium dihydrophosphate (KDP), Sitall, quartz glass, by using diamond cutter and abrasive diamond tools, are presented in the chapter. Kinematic schemes of ultra-precise machining of optical surfaces and the basic theoretical dependences for calculation of cutting layer thickness are considered. Recommended cutting modes and conditions are presented. The examples of diamond milling and abrasive processing on ultra-precise experimental stands and results of metrological control of treated surface quality parameters are also given.

Keywords High-accuracy machining · Optical materials · Diamond micromilling · Diamond grinding

1 Introduction

The traditional technology of treatment of the surface of elements made of optical materials provides diamond grinding with a successive reduction of abrasive grit and chemical mechanical polishing. The main disadvantages of traditional technology are poor process performance, complexity of automation and control, and

S. V. Grubiy (✉)
BMSTU, 5/1, 2-aya Baumanskaya Street, Moscow 105005, Russia
e-mail: grusv@yandex.ru

M. A. Shavva · V. V. Lapshin
VNIIINSTRUMENT, 49, B. Semenovskaya, Moscow 103027, Russia

A. A. Radionov et al. (eds.), *Proceedings of the 5th International Conference on Industrial Engineering (ICIE 2019)*, Lecture Notes in Mechanical Engineering,
https://doi.org/10.1007/978-3-030-22063-1_101

damage to the surface layer by abrasive particles. In Bauman Moscow State VNIIINSTRUMENT JSC, Resurs Tochnosti LLC in cooperation with other organizations carried out a set of technological researches and engineering developments aimed at increasing the productivity, accuracy, and quality of treatment of the surface of the elements made of optical materials by diamond edge and abrasive tools. Technological experimental studies were carried out on high-accuracy stands according to the diagram of flat surface milling by diamond single-cutter milling head and flat diamond grinding with the grinding wheel shaft tilted. Samples for treatment are made of optical materials: Sitall, quartz glass, and potassium dihydrogen phosphate. It is theoretically substantiated and experimentally confirmed that it is possible to create conditions for treatment that ensure cut layer thickness in the nanometer range providing that the mechanism of fragile interaction "tool-treated material" is changed to the plastic deformation [1–5]. The transition from brittle chipping to plastic deformation allows to obtain a surface with minimal damaged layer and roughness Ra less than 0.01 μm. The treated surface form error is ensured by the high-accuracy machine kinematics [6].

2 Diamond Single-Point Cutting

To ensure optical material plastic deformation in the cutting area, the diamond single-crystal tool shall have the following characteristics: front angle in the range of 0° to −35° [7]; cutting edge corner radius: 50–100 nm; tool blade top radius: 1–10 mm; rear angle: 7°–15°.

The cut layer thickness in course of the edge treatment depends on the cutting modes and parameters of the cutting tool. Figure 1 shows the dependencies of the cut layer thickness a on the longitudinal feed of the workpiece per one revolution of the tool S at 1 mm radius and 2 μm cutting depth, and Fig. 2 shows the above dependencies on cutting depth t at 1 mm top radius and 2 μm/rev workpiece feeding.

The analysis shows that the cut layer thickness decreases as the workpiece feeding and cutting depth decrease [8–14]. It has been experimentally proven that the cut layer thickness should not exceed 100–120 nm to ensure KDP.

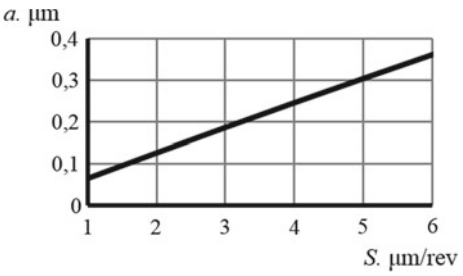

Fig. 1 Graph of dependence of the cut layer thickness on the workpiece feeding

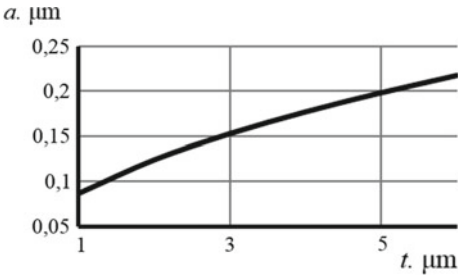

Fig. 2 Graph of dependence of the cut layer thickness on the cutting depth

Experimental studies on the treatment by a single-cutter diamond milling head were carried out on the high-accuracy experimental stand for diamond micromilling with the following constructional features: Stand spindle box and linear saddle are made on aerostatic bearings; the stand is mounted on antivibration mounts; the spindle box motor cooling system is provided.

The main parameters of the high-accuracy experimental stand are given in Table 1.

The kinematic diagram of treatment by an edge diamond tool on the high-accuracy experimental stand is shown in Fig. 3. The objects of research were workpieces made of potassium dihydrogen phosphate (KDP) with dimensions of 180 × 180 × 10 mm.

The parameters of the diamond cutter, cutting modes, and cut layer thickness are given in Table 2.

Leica DCM3D 3D profilometer was used to control the treated surface roughness. The treated surface profilogram is shown in Fig. 4. The treated surface roughness was Ra 3 nm, Rz 12 nm.

The form error of the treated flat surface of KDP workpiece was measured by the laser interferometer produced by the RAS Applied Physics Institute (Nizhny Novgorod). Figure 5 shows the treated surface interferogram. The flatness deviation was 280 nm. The treated part form error is determined by the machine slideway straightness error, poor alignment accuracy, and vibrations occurring during treatment [15].

Table 1 Parameters of high-accuracy experimental stand for diamond micromilling

No.	Parameter Name	Size
1.	The largest dimensions of the workpiece, mm	450 × 450
2.	Spindle speed range, min^{-1}	50–600
3.	Number of axles, pcs. *X*-axis—tangential saddle *C*-axis—spindle rotation	2
5.	Tangential saddle stroke, *X*-axis, mm	800
6.	Resolving power along *X*-axis, nm	1
7.	Feeding range along *X*-axis, mm/min	0.002–150

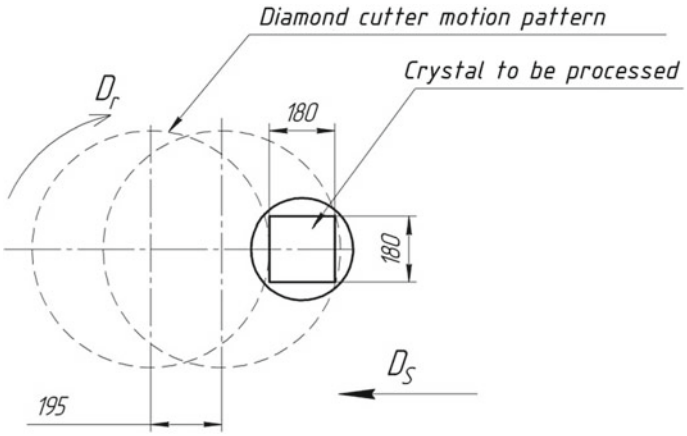

Fig. 3 Kinematic diagram of treatment on high-accuracy experimental stand for diamond micromilling

Table 2 KDP workpiece treatment modes

Parameter	Size
Single-cutter milling head R_{ml}, mm	325
Diamond cutter radius r, mm	1
Cutting depth t, μm	2
Feed per revolution S, μm/rev	2
Spindle speed n, rpm	340
Cut layer thickness a, nm	124

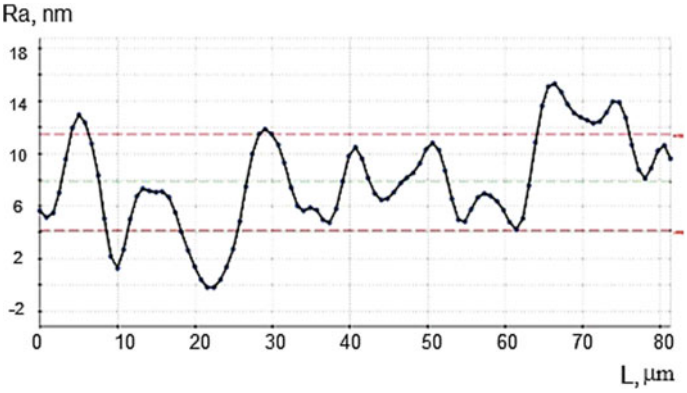

Fig. 4 KDP workpiece treated surface profilogram

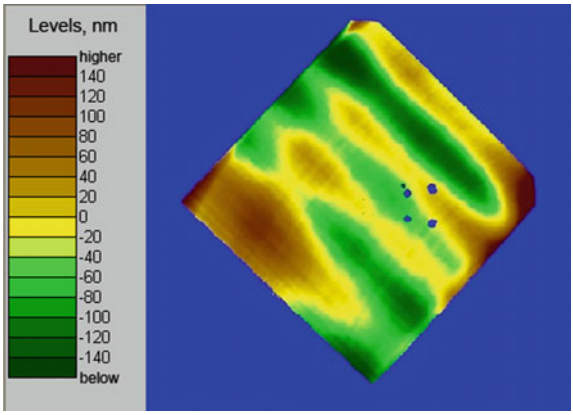

Fig. 5 KDP workpiece treated surface interferogram

Results of experimental studies on edge diamond blade treatment show that optical and microelectronics components made of potassium dihydrogen phosphate, silicon, and germanium can be treated with the roughness Ra that does not exceed 5 nm by providing plastic deformation conditions for the material in the cutting area [16–18].

3 Diamond Grinding

To ensure plastic deformation in course of the diamond grinding—the cut layer thickness in the nanometer range, the cutting tool shall have the following parameters: diamond bearing layer abrasive grit in the range of 2–3 μm; grain concentration in the diamond bearing layer—not less than 150%; use of organic bonds; periodic adjustment of the grinding wheel; it was also proposed to use the flat grinding diagram with the wheel shaft tilt in relation to face-plate spinning axis with workpieces—Fig. 6 [19]. In Fig. 5, the grinding wheel with radius R is tilted to an angle β and rotates at a frequency n_1. The workpiece circular feed at S_{prod} speed is set by the rotation speed n_2 of the rotary table with D_{zag} diameter. Cutting depth is indicated by t. The wheel transverse feed is carried out at S_{pop} speed. Changing the grinding wheel shaft tilt allows to change the direction of the crack development in the damaged layer. Optimum tilt of the wheel that provides plastic deformation of the material in the cutting area and minimum depth of the fractured layer (less than 50 nm) is experimentally confirmed and located in the range of 1°–3°. Table 3 provides parameters for calculating the cut layer thickness by single grain cutting when grinding with the wheel shaft tilted.

Figure 6 shows a graph of the dependency of the cut layer thickness by single grain cutting on the longitudinal feed. Calculations show that the cut layer thickness depends on the cutting modes, cutting tool parameters, and wheel shaft tilt. The kinematic diagram for treatment by diamond grinding wheel with shaft tilt (Fig. 7)

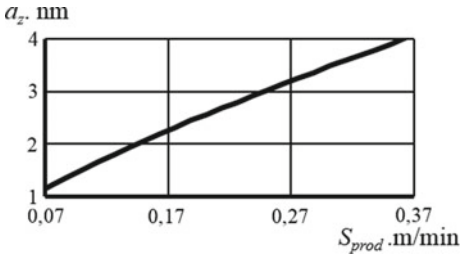

Fig. 6 Graph of dependence of the cut layer thickness by single grain cutting on longitudinal

Table 3 Parameters for calculating the cut layer thickness by single grain cutting

Parameter	Size
Coefficient that takes into account the grains in the bundle ε	0.5
Average diameter of diamond grain x, μm	2
Concentration of grains in diamond bearing layer K, %	100
Wheel rotation speed n_1, rpm	1000
Cutting depth t, μm	5
Width of diamond bearing layer B, m	0.01
Radius of grinding wheel R, m	0.05
Wheel shaft tilt β, deg	1.5

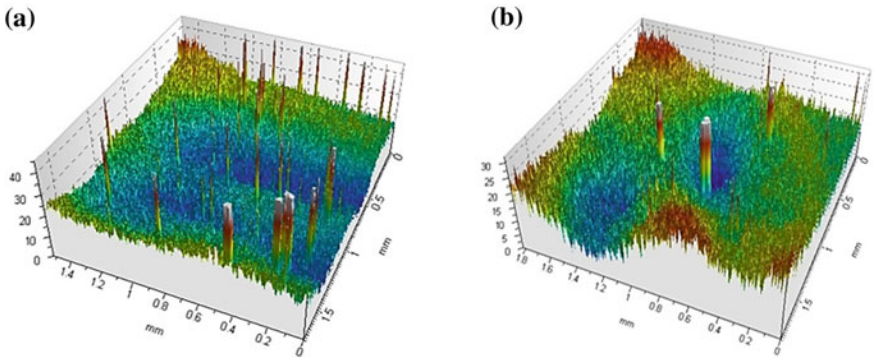

Fig. 7 Topograms of treated optical surfaces: **a** Sitall SO-115 M; **b** quartz glass KU1

was implemented on a high-accuracy experimental stand. The parameters of the stand are given in Table 4.

The structural features of the stand are: Workpiece spindle and grinding wheel spindle are based on gas-lubricated bearings, which provides the value of the operating surfaces radius runout not exceeding 0.5 μm and roughness not less than 100 N/μm; longitudinal and transverse saddles are made with porous choking for

Table 4 Parameters of the high-accuracy experimental stand to examine the optical surface grinding process

No.	Parameter Name	Size
1.	Frequency range of grinding spindle n_1, min^{-1}	50–3000
2.	Workpiece spindle speed range n_2, min^{-1}	0.01–100
3.	Longitudinal saddle stroke, Z-axis (cutting saddle), mm	100
4.	Tangential saddle stroke, *X*-axis, mm	200
5.	Number of axles, pcs. *X*-axis—tangential saddle *Z*-axis—longitudinal saddle (cut-in) *S*-axis—grinding wheel rotation; *S*1-axis—workpiece rotation	4
6.	Working feed of longitudinal saddle, mm/min	5–200
7.	Tangential saddle movement discretibility, μm	0.1
8.	Power of electric motor grinding wheel, kW	1

gas lubrication feeding and have additional damping by extra viscous liquid; the machine display system allows to set the value of the tool cutting within the accuracy of 0.1 μm.

The objects of research for diamond grinding were workpieces made of Sitall brand SO-115 M and quartz glass brand KU1. The workpiece treatment in course of the diamond grinding was carried out in the following modes: cutting depth t—1–2 μm, grinding wheel rotation speed n_1—1000 rpm, workpiece spindle speed n_2—0.2 rpm, and S_{prod} longitudinal feed—0.0075 m/min. The workpiece rotation diameter was 120 mm. Diamond wheel used for grinding: shape 12A2 45°, wheel dimensions: diameter—100 mm, height—21 mm, bore diameter—20 mm, diamond bearing layer width—6 mm, diamond bearing layer height—3 mm, ASM brand diamond powder with the abrasive grit of 3/2 microns, concentration—100%, and bond grade—B1.

Analysis of the experimental studies results shows that diamond grinding of optical materials allows to provide conditions for material plastic deformation in the cutting area and obtain the treated surface roughness Ra not less than 10 nm. In addition, the plastic material deformation in the cutting area and using of the grinding diagram with the wheel shaft tilted provide the reduction of the damaged layer depth to the value less than 50 nm. The fractured layer minimum depth allows to reduce the dispersion value directed to the treated optical surface of dispersion, and the general efficiency, durability, and accuracy of the instruments [20–22].

4 Conclusion

The obtained experimental data on diamond edge and abrasive treatment allow us to conclude that upon conditions of plastic deformation for optical materials in the cutting area, the treated surface roughness Ra is less than 10 nm, and the fractured

layer depth does not exceed 50 nm. The obtained quality parameters of the treated surfaces of KDP crystals, Sitalls, and quartz glass show that during treatment of the considered materials by diamond milling and grinding on high-accuracy machines, it is possible to minimize or exclude polishing operations from the technological process. The necessary recommendations for cutting tool parameters and treatment modes shall be observed to ensure plastic deformation of the optical material in the cutting area. At the same time, the treated surface form accuracy is ensured by kinematic accuracy of the equipment used and can reach up to 0.3 μm on the aperture 180 × 180 mm.

References

1. Xianqun H, Chaoshui X (2015) Specific energy as an index to identify the critical failure mode transition depth in rock cutting. Rock Mech Rock Eng 49:1461–1478
2. Masahiko Y, Sivanandam A, Matsumura T (2008) Critical depth of hard brittle materials on nano plastic forming. J Adv Mech Des Syst Man 2(1):59–70
3. Muhammad A, Mustafizur R, Wong Y (2011) Analytical modelling of ductile regime machining of tungsten carbide by end-milling. Int J Adv Man Techn 5:53–64
4. Bifano T, Fawcett S (1991) Specific grinding energy as an in process control variable for ductile-regime grinding. Prec Eng 4:256–262
5. Masahiko Y, Sivanandam A, Matsumura T (2008) Critical depth of hard brittle materials on nano plastic forming. J Adv Mech Des Syst Man 1:59–70
6. Borovskiy G, Shavva M, Grubiy S et al (2015) Ultraprecision machining of brittle optical materials. Rus Eng Res 91:883–889
7. Bifano T, DePiero D, Golini D (1993) Chemomechanical effects in ductile regime machining of glass. Prec Eng 4:238–247
8. Qiangguo W, Hang G, Zhijian P (2013) An experimental investigation on slicing of potassium dihydrogen phosphate crystal. J Eng Man 227:890–897
9. Zhang J, Zhang Y, Xu K (2008) Young's modulus surface and Poisson's ratio curve for tetragonal crystals. J Chem Cryst 17(5):1565–1573
10. Fang T, Lambropoulos J (2002) Microhardness and indentation fracture of potassium dihydrogen phosphate (KDP). J Am Cer Soc 85(1):174–178
11. Chunpeng L, Hang G, Jinghe W (2010) Mechanical properties of potassium dihydrogen phosphate single crystal by the nanoindentation technique. Mat Man Proc 25:740–748
12. Zhang Y, Zhang L, Liu M (2016) Revealing the mechanical properties of potassium dihydrogen phosphate crystals by nanoindentation. J Mat Res 31(8):1056–1064
13. Chen H, Dai Y, Zheng Z (2011) Effect of crystallographic orientation on cutting forces and surface finish in ductile cutting of KDP crystals. Mach Sci Techn An Int J 15:231–242
14. Hocheng H, Hsieh M (2004) Signal analysis of surface roughness in diamond turning of lens molds. Int J Mach Tools Man 44:1607–1618
15. Blake P, Scattergood R (1990) Ductile regime machining of germanium and silicon. J Am Cer Soc 73(4):949–957
16. Goel S, Luo X, Comley P (2013) Brittle-ductile transition during diamond turning of single crystal silicon carbide. Int J Mach Tools Man 65:15–21
17. Yan J, Yoshino M, Kuriagawa T (2001) On the ductile Machining of silicon for micro electro-mechanical system (MEMS). Opto-electronic and optical applications. Mat Scien Eng 297:230–234

18. Zaharevich E, Lapshin V, Shavva MA et al (2016) The Experimental Determination of the Ductile-Fracture Transition Boundaries when Cutting Brittle Materials. News of High Ed Inst Eng 7:64–71
19. Shavva M (2017) The Methods of calculation of cutting forces for diamond grinding of brittle optical materials. News High Ed Inst Eng 2:61–69
20. Inkson B, Wu H, Steer T et al (2001) 3D mapping of subsurface cracks in alumina using FIB. Mat Res Soc 649:Q.7.7.1–Q.7.7.6
21. Salvati E, Sui T, Lunt A, Korsunsky A (2016) The effect of eigenstrain induced by ion beam damage on the apparent strain relief in FIB-DIC residual stress evaluation. Mat and Des 92:649–658